



# Synthesis and characterization of MCM-41-supported $\text{Ba}_2\text{SiO}_4$ base catalyst

Quanchang Li<sup>a</sup>, Suzanne E. Brown<sup>a</sup>, Linda J. Broadbelt<sup>a,\*</sup>,  
Jian-Guo Zheng<sup>b</sup>, N.Q. Wu<sup>c</sup>

<sup>a</sup> Department of Chemical Engineering, Center for Catalysis and Surface Science, Northwestern University,  
2145 Sheridan Road, Evanston, IL 60208-3120, USA

<sup>b</sup> Department of Materials Science and Engineering, Electron Probe Instrumentation Center, Northwestern University,  
Evanston, IL 60208, USA

<sup>c</sup> Department of Chemistry, Keck Interdisciplinary Surface Science Center, Northwestern University, Evanston, IL 60208, USA

Received 26 September 2002; received in revised form 20 January 2003; accepted 23 January 2003

## Abstract

A novel MCM-41-supported base catalyst, Ba-MCM-41, was synthesized with a modified impregnation method.  $\text{Ba}_2\text{SiO}_4$  was synthesized on the MCM-41 pore wall as confirmed by characterization using X-ray diffraction, X-ray photoelectron spectroscopy, X-ray fluorescence,  $\text{N}_2$  adsorption,  $^{29}\text{Si}$  MAS NMR and transmission electron microscopy. It was also demonstrated that a highly ordered Ba-MCM-41 catalyst with high barium loading (4.1–25.2 wt.%) and dispersion was obtained using this method. The basicity of the catalyst, which was characterized according to the binding energy of O 1s, was increased with increasing amounts of barium in the catalyst.

© 2003 Elsevier Science Inc. All rights reserved.

**Keywords:** Barium; MCM-41; Barium silicate; Impregnation

## 1. Introduction

The discovery [1,2] of MCM-41 mesoporous molecular sieves has sparked much research into developing new materials with uniform pore size and shape that have very high surface area and adsorption capacity. The development of such materials is of great importance in many areas of modern science and technology [3–6]. These materials are best appreciated in systems where mo-

lecular recognition is needed, e.g., shape-selective catalysis, selective adsorption and separation processes, chemical sensors, and nanotechnology. Ordered mesoporous oxides of the MCM-41 type have been used and evaluated with respect to their catalytic properties as supports, mainly for metal particles or molecular catalysts. However, they might also be useful, with possibly even broader applications, for the preparation of supported base metal oxides that are important in many catalytic reactions [7].

A common method for preparing supported base metal oxides is impregnation, where a porous support is repeatedly dipped into a solution containing a desired catalytic agent. It is often desirable to

\* Corresponding author. Tel.: +1-847-491-5351/7398; fax: +1-847-491-3728.

E-mail address: [broadbelt@northwestern.edu](mailto:broadbelt@northwestern.edu) (L.J. Broadbelt).

apply the agent uniformly in a predetermined quantity to a preset depth of penetration, but penetration of the liquid solution into the porous support is hindered by air trapped in the pores. In addition, when calcination is employed, the exiting gas will remove the liquid at the exit of the pores, resulting in formation of some catalytic particles on the external surface of the porous material. As a result, several groups [8–10] have reported many small particles that were formed on the external surface of porous materials if conventional impregnation was used to prepare catalysts with metal oxides supported on the surface of a mesoporous material. Generally, various techniques like pressurizing, vacuum treatment, or acoustic activation have been proposed to remove gas trapped in the pores. Therefore, these techniques can be used to modify a typical impregnation method and facilitate the impregnation process.

In the present paper, we report the synthesis of a highly dispersed basic Ba-MCM-41 catalyst by a modified impregnation method which employed reduced pressure. While the preparation of BaO particles supported on MCM-41 has been reported [11], our preparation method resulted in the formation of BaSiO<sub>4</sub> on the framework of MCM-41. To the best of our knowledge, this synthesis of a Ba<sub>2</sub>SiO<sub>4</sub> phase on the framework of MCM-41 was achieved for the first time.

## 2. Experimental

### 2.1. Synthesis

Tetramethylammonium hydroxide (TMAOH), cetyltrimethylammonium bromide (CTAB), fumed silica and barium nitrate were obtained from Aldrich. Distilled water was used for all syntheses.

The material MCM-41 was synthesized according to the procedure reported in the literature [15]. The molar ratio of the components was as follows: Si:0.25 CTAB:0.2 TMAOH:40 H<sub>2</sub>O. Once the silica was added, the solution was stirred for two hours. The resulting gel was then transferred into a Teflon-lined autoclave and aged at 150 °C for 48 h. After aging, the gel was filtered, washed several times with distilled water, and dried at

room temperature. Once dry, the gel was then calcined at 550 °C (heating rate of 1 °C/min) for 4 h in order to remove the organic template and create the hollow porous structure. The calcined MCM-41 was characterized by low-angle X-ray diffraction (XRD), N<sub>2</sub> sorption and transmission electron microscopy (TEM).

The MCM-41-supported Ba<sub>2</sub>SiO<sub>4</sub> catalyst was first obtained by a modified wet impregnation method. 7.5 g of barium nitrate were dissolved in 100 ml distilled water. 0.9 g MCM-41 were added to the barium nitrate solution. After stirring for 0.5 h under reduced pressure (achieved via water aspiration) at room temperature, the solid was filtered from the solution and dried at room temperature. Final calcination was carried out at 600 °C for 2 h (heating rate of 1 °C/min), and the Ba-MCM-41 catalyst was obtained. Other catalysts containing different amounts of barium were obtained with the same method but varying the barium nitrate concentration (1.0, 2.5, 5.0 g barium nitrate/100 ml H<sub>2</sub>O). These catalysts were fully characterized by XRD, X-ray photoelectron spectroscopy (XPS), X-ray fluorescence (XRF), N<sub>2</sub> sorption, <sup>29</sup>Si MAS NMR and TEM.

### 2.2. Characterization

*X-ray diffraction:* The XRD patterns were collected by a Rigaku DMAX-A diffractometer with CuK $\alpha$  radiation ( $\lambda = 1.5418 \text{ \AA}$ ),  $\theta$ - $2\theta$  geometry and a scintillation detector. Each diffraction pattern was recorded at a step of 0.01° and 1 s per step. All measurements were made at room temperature.

*X-ray photoelectron spectroscopy:* XPS spectra were obtained by using an Omicron ESCA Probe, which was equipped with an electron flood gun. The AlK $\alpha$  radiation (1486.6 eV) was used as an excitation source. The binding energy scale was calibrated with respect to the adventitious carbon (C 1s) at 284.8 eV.

*X-ray fluorescence:* Elemental analysis was carried out on a Bruker S4 Explorer XRF analyzer.

*N<sub>2</sub> sorption:* A Tristar 3000 N<sub>2</sub> sorption apparatus was used to collect the BET data. The samples were degassed at 250 °C overnight before the measurements were taken. The BET surface area

was calculated based on the adsorption data in the relative partial pressure range of 0.05–0.2. Pore size distributions were determined based on the Barrett–Joyner–Halender (BJH) adsorption curve.

<sup>29</sup>Si magic angle spinning (MAS) solid-state NMR: <sup>29</sup>Si spectra were recorded on a Varian VXR 300 spectrometer using zirconia rotors of 5 mm in diameter spinning at 4 kHz in air. <sup>29</sup>Si NMR spectra were acquired at 59.57 MHz by xpolar pulse sequence, with a delay time of 10 s. 1440 scans were sufficient to give high quality spectra. Chemical shifts are given as  $\delta$  from the external polydimethylsilane (PDMS) standard.

*Transmission electron microscopy*: TEM was carried out on a Hitachi HF-2000 TEM, which is capable of atomic resolution with a high-brightness cold cathode field emission gun operated at 200 kV. Samples were prepared by suspending porous materials in ethanol followed by sonication for 30 min in an ultrasonic bath. The suspension was dropped onto a copper grid and allowed to dry.

### 3. Results and discussion

The MCM-41 host was synthesized with cetyltrimethylammonium bromide (CTAB) as the template according to the procedure reported in the literature [12]. The calcined MCM-41 was characterized by low-angle XRD measurements (which exhibit the characteristic reflections of high-quality hexagonal mesostructures, Fig. 1), N<sub>2</sub> sorption studies (Table 1) and TEM (Fig. 2). The Brunauer–Emmett–Teller (BET) surface area of the empty MCM-41 was 986 m<sup>2</sup>/g, and the pore-size distribution centered at 3.2 nm was calculated from BJH theory on the basis of N<sub>2</sub> adsorption data.

For the introduction of barium species onto the MCM-41 support, a modified wet impregnation method was employed under reduced pressure (achieved via water aspiration). As discussed in Section 1, gas adsorbed in the MCM-41 pores will hinder the deposition of barium nitrate on the pore walls. As a result, particles will be deposited on the external surface of the MCM-41. To prevent this, we used reduced pressure to remove substantial amounts of gas from the pore structure, facilitating the penetration of the barium nitrate solution in the

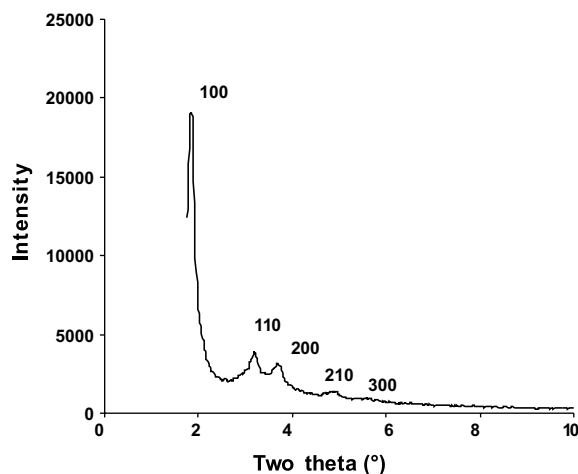


Fig. 1. Powder XRD pattern of the calcined form of MCM-41.

Table 1  
XRF and N<sub>2</sub> adsorption results of MCM-41 and Ba-MCM-41 catalysts

	Barium (wt. %)	$S_{\text{BET}}$ (m <sup>2</sup> /g)	Pore size (nm)	Pore volume (ml/g)
MCM-41	0	986	3.2	0.947
Ba- MCM-41	4.1	768	3.1	0.705
	8.9	698	3.1	0.638
	15.3	582	3.0	0.526
	25.2	568	3.0	0.516

pores. The solid was filtered from the solution and dried at room temperature. Final calcination was carried out at 600 °C for 2 h (heating rate of 1 °C/min), and the Ba-MCM-41 catalyst was obtained.

To confirm the formation of the Ba<sub>2</sub>SiO<sub>4</sub> phase, the calcined catalyst powder with the highest barium loading achieved (25.2 wt.% Ba) was characterized by XRD (Fig. 3). Fig. 3a and b shows the XRD pattern of the MCM-41 supported Ba<sub>2</sub>SiO<sub>4</sub> base catalyst in the low-angle region ( $2\theta = 1.75\text{--}10^\circ$ ) and the high-angle region ( $2\theta = 15\text{--}35^\circ$ ), respectively. It is observed that the highly ordered hexagonal pore structure of MCM-41 is still intact, while the intensity of the characteristic XRD reflections of MCM-41 (Fig. 1) is reduced for the MCM-41 supported Ba<sub>2</sub>SiO<sub>4</sub> catalyst. This can be attributed to modification of the pore wall with Ba<sub>2</sub>SiO<sub>4</sub>, which reduces the scattering contrast between the pores and the walls of the

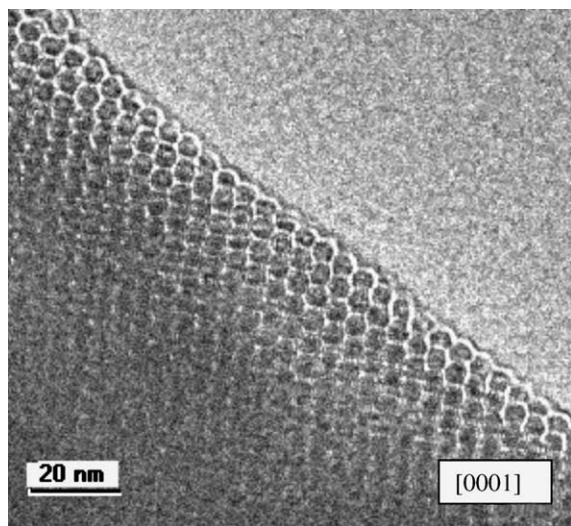


Fig. 2. TEM images of calcined MCM-41 viewed through the pore axis [0001].

molecular sieve [13]. The tiny reflections ( $2\theta = 26.1^\circ, 29.7^\circ, 30.4^\circ$  and  $30.9^\circ$ ) of the  $\text{Ba}_2\text{SiO}_4$  phase in the XRD pattern (high-angle region) of the catalyst indicate the formation of  $\text{Ba}_2\text{SiO}_4$ . It is noteworthy that there were no clear reflections found in the XRD patterns of the MCM-41 supported  $\text{Ba}_2\text{SiO}_4$  catalysts in which the Ba content was less than 25.2 wt.%. This implies that lower Ba contents will not result in the formation of continuous crystalline  $\text{Ba}_2\text{SiO}_4$  on the framework of MCM-41 or that the size of crystalline  $\text{Ba}_2\text{SiO}_4$  is

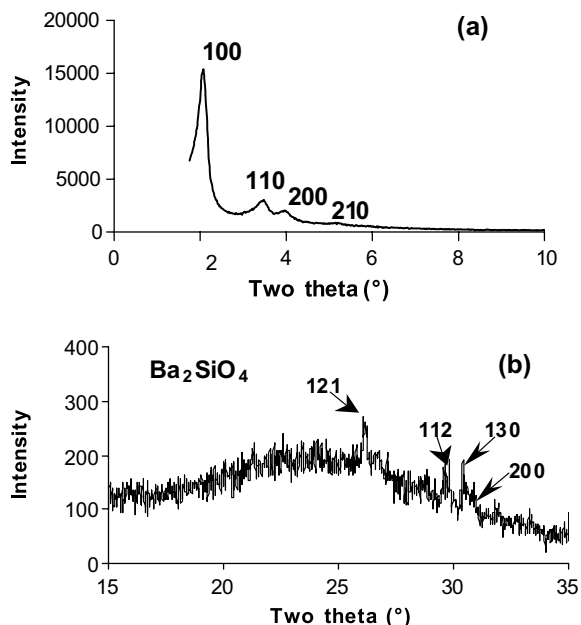


Fig. 3. XRD patterns of the MCM-41-supported  $\text{Ba}_2\text{SiO}_4$  catalyst.

too small to be detected by XRD. It is interesting that instead of the (130) plane of the  $\text{Ba}_2\text{SiO}_4$  phase, the (121) plane shows the highest reflection peak in the XRD pattern (Fig. 4b) [14]. This may be due to MCM-41 limiting the growth of the  $\text{Ba}_2\text{SiO}_4$  phase and the (121) plane growing on the pore wall along the axis of the hexagonal pores of MCM-41.

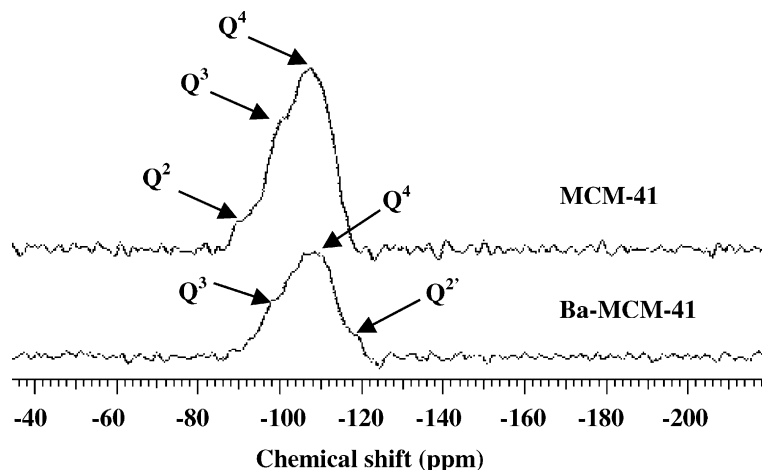


Fig. 4.  $^{29}\text{Si}$  solid-state MAS NMR of pure MCM-41 and the MCM-41-supported  $\text{Ba}_2\text{SiO}_4$  catalyst.

Evidence of the  $\text{Ba}_2\text{SiO}_4$  phase, which formed during the modification of the silica MCM-41 surface, was also obtained from magic angle spinning (MAS) solid-state  $^{29}\text{Si}$  NMR (Fig. 4). Three different coordinations of Si,  $\text{Q}^4$  (Si-nuclei  $(\text{OSi})_4$ ),  $\text{Q}^3$  (Si-nuclei  $(\text{OSi})_3(\text{OH})$ ) and  $\text{Q}^2$  (Si-nuclei  $(\text{OSi})_2(\text{OH})_2$ ), were found at  $-108$ ,  $-101$  and  $-92$  ppm in the spectrum of pure MCM-41, which is in agreement with literature results [15]. After modification of the MCM-41 surface by Ba impregnation, the  $\text{Q}^2$  species peak shifts from  $\delta = -92$  to  $-119$  ppm. This is because the surface hydroxyl groups of the  $\text{Q}^2$  (Si-nuclei  $(\text{OSi})_2(\text{OH})_2$ ) species reacted with the barium source and formed the  $\text{Q}^{2'}$  (Si-nuclei  $(\text{OSi})_2\text{O}_2\text{Ba}$ ) species at  $-119$  ppm.

TEM images of the MCM-41 supported  $\text{Ba}_2\text{SiO}_4$  catalyst (25.2 wt.% Ba) are shown in Fig. 5. These images reveal that the hexagonally ordered mesostructure of the MCM-41 host material was unaffected by surface modification with  $\text{Ba}_2\text{SiO}_4$ . No crystalline particles were found on the external surface of the MCM-41 framework, indicating that all barium sources were dispersed inside the mesostructure homogeneously. The TEM images also show a much stronger contrast than the pure silica MCM-41 (Fig. 2), which might be partially attributed to the presence of barium as a stronger scatterer/absorber in a homogeneous distribution.

$\text{N}_2$  adsorption results (Table 1) show that the BET surface area is still above  $568 \text{ m}^2/\text{g}$  when the barium content was increased to 25.2 wt.%, and the average pore size decreases from 3.2 to 3.0 nm due to the formation of  $\text{Ba}_2\text{SiO}_4$  on the pore walls. In comparison to literature results [11] in which only 10% by weight BaO particles formed in the porous structure, the deposition of BaO clusters reduced the pore space, resulting in a decrease of the BET surface area from 982 to  $535 \text{ m}^2/\text{g}$ . The decrease in our surface area was comparable for a significantly higher Ba content, suggesting that the modified impregnation method more successfully dispersed Ba on the framework of MCM-41. This might be due to the use of a vacuum system that helped remove all of the gas from the porous structure of MCM-41 and the use of a barium nitrate solution that dispersed Ba into MCM-41 homogeneously before calcination.

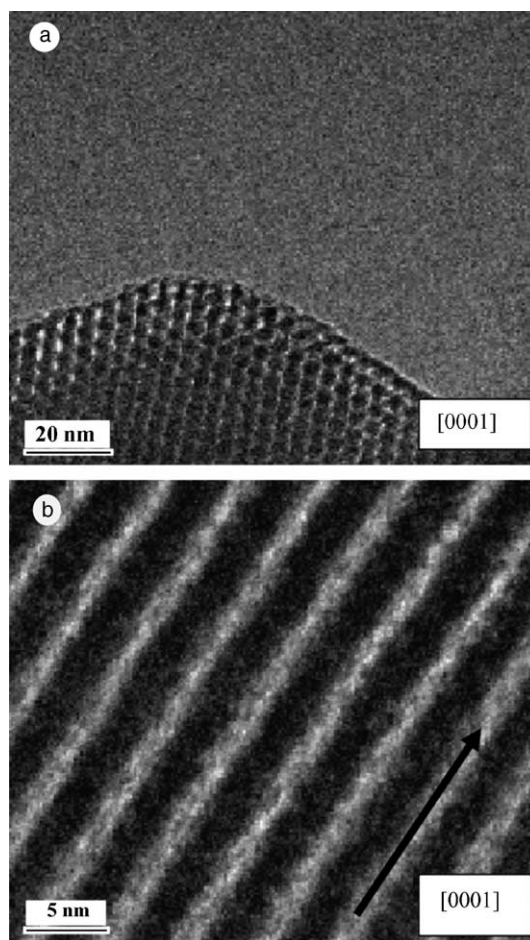


Fig. 5. TEM images of calcined Ba-MCM-41 catalyst viewed (a) through the pore axis  $[0001]$  and (b) along the pore channels ( $[0001]$  direction depicted by arrow).

XPS measurements were carried out on the MCM-41-supported  $\text{Ba}_2\text{SiO}_4$  catalyst to confirm the formation of barium silicate and to determine the surface basicity. Fig. 6a shows the Si 2p binding energy in both MCM-41 and  $\text{Ba}_2\text{SiO}_4$ . The full width at half maximum of the Si 2p peaks increased with increasing Ba content, and the degree of asymmetry also increased. Deconvolution of the peaks through fitting revealed two distinct Si 2p binding energy peaks, indicating the existence of two different Si species: the main peak at 104.1 eV is attributed to the  $\text{SiO}_2$  of MCM-41, while the other small peak at 102.2 eV likely arises from the new  $\text{Ba}_2\text{SiO}_4$  species. In addition, XPS spectra also

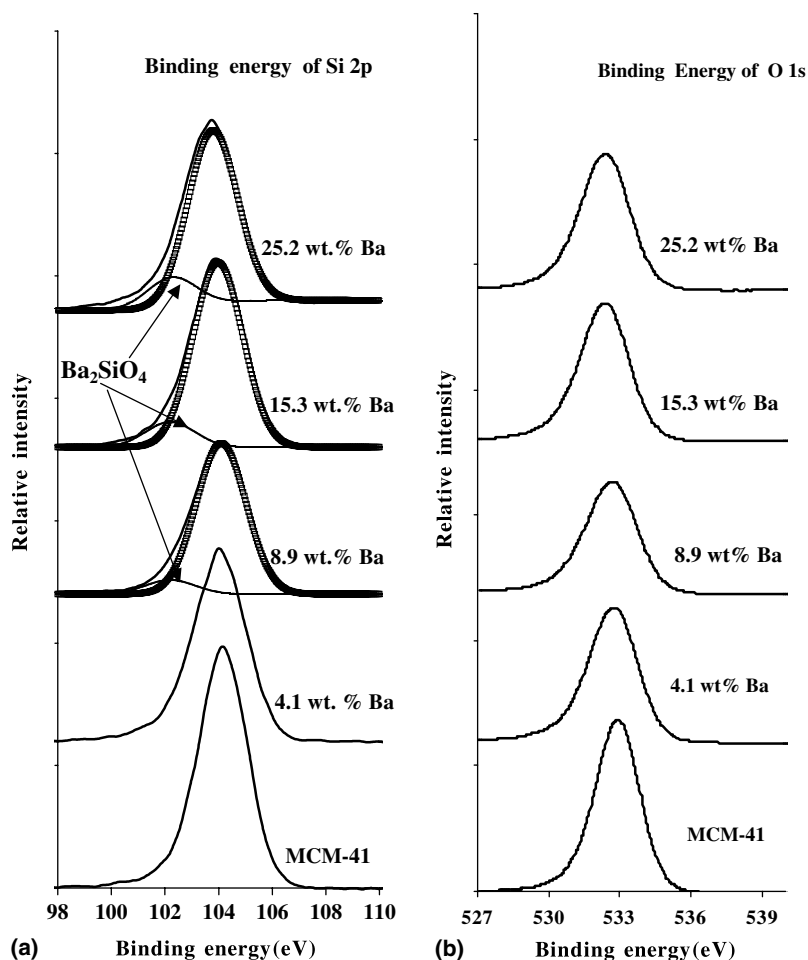


Fig. 6. XPS spectra of pure MCM-41 and the MCM-41-supported  $Ba_2SiO_4$  base catalyst focusing on: (a) Si 2p and (b) O 1s peaks.

provide very important information about changes in the surface basicity (Fig. 6b). Since the binding energy of O 1s decreases from 533.0 to 532.5 eV after formation of  $Ba_2SiO_4$  on the framework of MCM-41, this means that the Lewis basicity of the surface increased after the modification of MCM-41 with  $Ba_2SiO_4$ .

#### 4. Conclusions

Although ordered mesoporous MCM-41 materials have been used and evaluated with respect to

their catalytic properties as supports, the work reported in those publications [7,10,11,13,16] was undertaken with the goal of creating highly dispersed oxide species using ordered mesoporous supports. The synthesis of a highly dispersed basic species,  $Ba_2SiO_4$ , on the framework of MCM-41 is reported for the first time to the best of our knowledge. The combined results of XRD, XPS, XRF, TEM, MAS NMR and  $N_2$  adsorption have confirmed the existence of a  $Ba_2SiO_4$  phase on the framework of MCM-41. The catalyst basicity could be improved by changing the Ba content of the catalysts. Further investigations of the process

of surface modification of MCM-41 with different basic species and catalytic applications of these materials are underway.

### Acknowledgements

The authors are grateful for the support of the CAREER Program of the National Science Foundation (CTS-9623741). Prof. Snurr and Prof. Kung are acknowledged for offering laboratory equipment. Dr. Kai Zhang is acknowledged for helpful discussions on XRD.

### References

- [1] C.T. Kresge, M.E. Leonowicz, W.J. Roth, J.C. Vartuli, J.S. Beck, *Nature* 359 (1992) 710.
- [2] J.S. Beck, J.C. Vartuli, W.J. Roth, M.E. Leonowicz, C.T. Kresge, K.D. Schmitt, C.T.W. Chu, D.H. Olson, E.W. Sheppard, S.B. McCullen, J.B. Higgins, J.L. Schlenker, *J. Am. Chem. Soc.* 114 (1992) 10834.
- [3] T.J. Barton, L.M. Bull, W.G. Klemperer, D.A. Loy, B. McEnaney, M. Misono, P.A. Monson, G. Pez, G.W. Scherer, J.C. Vartuli, O.M. Yaghi, *Chem. Mater* 11 (1999) 2633.
- [4] Y. Ma, W. Tong, H. Zhou, L. Suib, *Micropor. Mesopor. Mater.* 37 (2000) 243.
- [5] K. Cheetham, G. Férey, T. Loiseau, *Angew. Chem. Int. Ed. Engl* 38 (1999) 3269.
- [6] P. Behrens, *Adv. Mater.* 5 (1993) 127.
- [7] F. Schüth, A. Wingen, J. Sauer, *Micropor. Mesopor. Mater.* 44–45 (2001) 465.
- [8] A. Bourlinos, A. Simopoulos, N. Boukos, D. Petridis, *J. Phys. Chem. B* 105 (2001) 7432.
- [9] D. Lensveld, J. Mesu, A. Dillen, K. Jong, *Micropor. Mesopor. Mater.* 44–45 (2001) 401.
- [10] R.S. Mulukutla, K. Asakura, T. Kogure, S. Namba, Y. Iwasawa, *Phys. Chem. Chem. Phys.* 1 (1999) 2027–2032.
- [11] S. Jaenicke, G.K. Chuah, X.H. Lin, X.C. Hu, *Micropor. Mesopor. Mater.* 35–36 (2000) 143.
- [12] R. Mokaya, *J. Phys. Chem. B* 104 (2000) 8279–8286.
- [13] B. Marler, U. Oberhagemann, S. Vortmann, H. Gies, *Micropor. Mesopor. Mater.* 6 (1996) 375.
- [14] H. Uchikawa, K. Tsukiyama, *ISIS Annual Report* 73 (1965) 106.
- [15] B.H. Wouters, T. Chen, M. Dewilde, P.J. Grobet, *Micropor. Mesopor. Mater.* 44–45 (2001) 453–457.
- [16] T. Abe, Y. Tachibana, T. Uematsu, M. Iwamoto, *J. Chem. Soc. Chem. Commun.* (1995) 1617.